

ORIGINAL RESEARCH

Open Access



Gas permeability and emission in unsaturated vegetated landfill cover with biochar addition

Junjun Ni¹, Jingsong Zhou¹, Yuchen Wang² and Haowen Guo^{2*} 

Abstract

Plant–biochar interaction has been recognized to affect the hydraulic properties of landfill cover soils, while its influence on landfill gas emission is rarely studied. This study investigated the coupled effects of biochar and vegetation on gas permeability and emission in unsaturated landfill cover through an integrated theoretical modelling and laboratory investigation. First, a gas permeability model was developed for vegetated coarse-grained soils with biochar addition. Then, a well-instrumented laboratory column test and two tests from the literature, considering bare, grass, biochar and grass + biochar conditions, were used for model validation. Finally, a numerical parametric study was conducted to investigate the influence of root growth and drought conditions on the gas emission rate. Results showed that the developed model can satisfactorily capture the gas permeability of unsaturated soils at various degrees of saturation. The lowest water retention capacity, the highest gas permeability and gas emission rate after 24 months of growth were observed in the grassed column. However, adding biochar in vegetated soils can maximize the water retention capacity and decrease the gas permeability, resulting in the lowest gas emission rate. The measured gas emission rates for the four cases meet the recommended value by the design guideline. The parametric study showed that the increased root depth from 0.2 m to 0.4 m improved the gas emission rate by 170% in the grass case but decreased by 97% in the grass + biochar case. Under the severe drought condition with soil suction around 500 kPa, the gas emission rate in the grassed case exceeded the design value by 18%, while those in the biochar cases were far below the allowable value. Therefore, peanut shell biochar should be considered to amend the grassed landfill cover using coarse-grained soils as it can significantly improve engineering performance in reducing gas emissions under extreme drought conditions.

Highlights

1. A new gas permeability model was developed for vegetated soil with biochar.
2. Grassed soil with decay roots had the largest gas permeability at any water content.
3. Biochar–grass interaction leads to the lowest gas permeability.
4. Gas emission rate decreased with deeper root depth in biochar–grass case.
5. Biochar can reduce gas emission rate even under drought condition.

Handling Editor: Lukáš Trakal.

*Correspondence:

Haowen Guo
hguoce@ust.hk

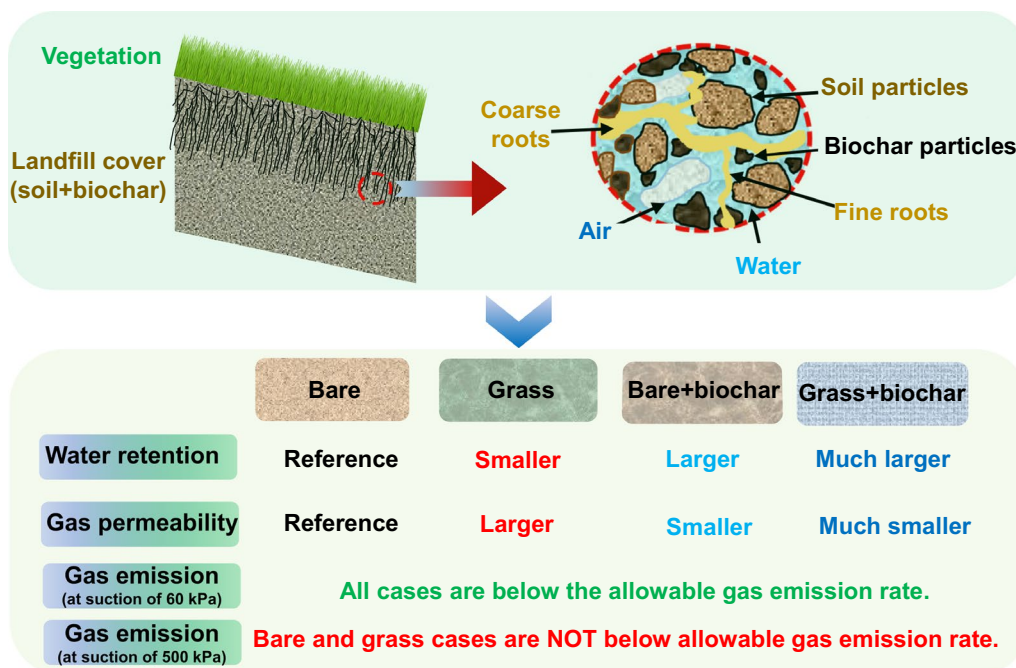
Full list of author information is available at the end of the article



© The Author(s) 2023. **Open Access** This article is licensed under a Creative Commons Attribution 4.0 International License, which permits use, sharing, adaptation, distribution and reproduction in any medium or format, as long as you give appropriate credit to the original author(s) and the source, provide a link to the Creative Commons licence, and indicate if changes were made. The images or other third party material in this article are included in the article's Creative Commons licence, unless indicated otherwise in a credit line to the material. If material is not included in the article's Creative Commons licence and your intended use is not permitted by statutory regulation or exceeds the permitted use, you will need to obtain permission directly from the copyright holder. To view a copy of this licence, visit <http://creativecommons.org/licenses/by/4.0/>.

Keywords Plant–biochar interaction, Gas permeability model, Gas emission, Numerical simulation

Graphical abstract



1 Introduction

The generation of municipal solid waste (MSW) has increased rapidly in recent years worldwide. Landfilling has been one of the main alternatives for disposing of MSW. Even though different approaches (e.g., recycling, recovery and reuse) have been developed to manage MSW, landfilling is still the most common method, especially in developing countries (Osra et al. 2021). Over time, the decomposition of MSW in landfill can generate a large amount of landfill gas, including methane and carbon dioxide, which are the main sources of greenhouse gases (Nguyen et al. 2019). Final landfill covers are commonly used as barriers between MSW and the atmosphere. The purpose of the final cover is to reduce water infiltration and minimize gas emissions (Ng et al. 2016a). Hence, the gas permeability of cover materials is of great importance in assessing the performance of earthen landfill cover. From engineering perspectives, low gas permeability is desired to reduce the emission of methane and carbon dioxide into the atmosphere. Landfill cover is normally in an unsaturated state due to the soil-atmosphere interactions. Gas permeability of unsaturated soils is affected by soil water content and

compacting dry densities (Wickramarachchi et al. 2011; Hamamoto et al. 2011). With the decrease in soil water content and increase in soil dry density, gas permeability increases (Garg et al. 2019).

Vegetation is commonly planted on the top of landfill covers for aesthetical and ecological purposes. Recently, it has been revealed that vegetation growth can help remove rainfall infiltrated water from the cover surface through evapotranspiration (Ng et al. 2016b). During the early stage of vegetation growth, active roots can reduce water infiltration by occupying soil pore space (Scholl et al. 2014). However, the infiltration rate for ageing plants is quite often increased (Vergani and Graf 2015) due to the formation of macropores from root decay (Ghestem et al. 2011). It can be easily deduced that plant root-induced changes in soil pore structure can also affect the gas permeability of unsaturated soils. Indeed, Zhan et al. (2016) conducted a field test and found that the active growth of plant roots in loosely compacted silt caused a gradual decrease in gas permeability by about one order of magnitude during the first few months. Recently, Ni et al. (2019) investigated the gas permeability variations of unsaturated soils planted

with a grass species over a two-year growth period. The results showed that after two years, the gas permeability of grass-covered soil was up to one order of magnitude higher than that in the bare soil. It is concluded that the ageing plant may not be beneficial for minimizing gas emissions in final landfill covers.

In order to promote the performance of vegetation, biochar is commonly applied in the field to improve soil fertility and engineering properties (Kumar et al. 2022; Ng et al. 2022a; Yan et al. 2022). Biochar is pyrolyzed from various wastes and feedstocks (e.g., pig manure, wood, crop residues and poultry litter) under high temperatures and low oxygen conditions (Kumar et al. 2019). It is an environmentally friendly soil amendment which can supply nutrients (e.g., N and K) to plants (Zornoza et al. 2016; Hossain et al. 2020), improve soil water retention capacity and alter microbial communities (Moore et al. 2018). As biochar has a porous structure and large specific area (Lehmann and Joseph 2009), it can change pore-size distribution and soil bulk density (Major et al. 2010) and hence affect soil hydraulic properties (Wong et al. 2017, 2022). Intuitively, biochar also affects the gas permeability of soils due to its highly porous structure (Sun et al. 2013; Nan et al. 2021). The application of biochar to loose soil can increase its gas permeability. However, Garg et al. (2019) revealed that adding biochar in compacted soil decreased gas permeability significantly compared with that of bare soil. Gas permeability increased linearly with soil suction in a semi-log scale, regardless of the biochar content. Garg et al. (2021) also found that 5% biochar was the most effective in reducing gas permeability when the degree of compaction increased from 65% to 95% at a low suction range (<200 kPa).

By considering soil–plant–biochar interactions, soil hydraulic properties differ from those with only biochar addition or vegetation. Root growth is mainly affected by temperature (Maeght et al. 2015), moisture gradient (Kobayashi et al. 2007), nutrients (Zornoza et al. 2016) and soil density (Grzesiak et al. 2002). Biochar can modify water-holding capacity and thus soil moisture content, affecting the growth conditions of the plant. Moreover, biochar contains various nutrients (e.g., N, P and K), which are slowly released into soil pores to benefit root proliferation (Ni et al. 2018; Guo et al. 2023). Ni et al. (2020) found that after 2 years of growth, the saturated water permeability of grassed soil with biochar was 16 times smaller than that without biochar. The presence of biochar could delay the root decay process in vegetated soils. A recent study by Ng et al. (2022a) revealed that the rainfall influence depth and factor of safety of vegetated slopes without biochar were about 100% deeper and 60% lower than the case with biochar, respectively. Until now,

even though there are some studies about the gas permeability of soils with only biochar addition or plant, the effectiveness of soil–plant–biochar interactions on gas permeability and gas emission is rarely studied. Up to now, there is no theoretical model yet to capture the gas permeability of unsaturated rooted soils considering biochar addition.

This study investigated the influence of soil–plant–biochar interactions on gas permeability and emission through integrated theoretical modelling and experimental investigation. First, a new gas permeability model for vegetated coarse-grained soil with biochar was developed, considering various root decay rates. The model can consider the influence of biochar and plant roots on pore structure in the long-term run. Then, a laboratory column test with grass and biochar was carried out to validate the performance of the new model. Finally, a numerical parametric study was conducted to explore the effects of soil–plant–biochar interactions on gas emission rate in the earthen landfill covers using the Air/W software.

1.1 Development of the new and simple gas permeability model

Recently, Ng et al. (2022a) developed a water retention model for vegetated coarse-grained soil with biochar. The model is expressed as follows:

$$S_r = \left[1 + \left(\frac{se^{m_4}}{m_3} \left(\frac{C_m}{D_m} \eta + 1 \right)^{-m_5} \right)^{m_2} \right]^{-m_1}. \quad (1)$$

In this equation, S_r (–) is the degree of saturation of the soil, s (kPa) is the matric suction. m_1 (–), m_2 (–), m_3 (kPa) and m_4 (–) are the model parameters. m_1 and m_2 determine the shape of a soil water retention curve (SWRC; van Genuchten 1980), while m_3 and m_4 are related to the air-entry value (AEV, α) of the soil ($\alpha = \frac{m_3}{e^{m_4}}$). m_5 (–) is a soil parameter for describing the effects of pore structure on AEV. The void ratio has a negligible impact on SWRC at a high suction range. Hence, the product, $m_1 m_2 m_4$, can be set to 1 (Gallipoli et al. 2003). C_m (–) is a soil parameter describing the biochar effects on the pore structure, and η (%) is biochar content. D_m (–) is a microstructural state variable of bare soil. e is the void ratio for the soil.

The void ratio is an essential soil parameter that reflects not only the soil-pore structure but also soil density. However, the void ratio for the soil with biochar and plant relied on the laboratory measurement in Ng et al. (2022a), which takes time and is not accurate enough. In addition, no available equation for void ratio considering

both biochar amendment and root occupation is derived in their work.

In this study, a simple method for calculating the void ratio of biochar-amended soil, e_i (-) is suggested as follows:

$$e_i = \frac{e_s + V_r e_b}{1 + V_r}, \tag{2}$$

where e_s (-) and e_b (-) are the void ratios of the soil and biochar, respectively. V_r (-) is the volume ratio of biochar-soil solid and can be expressed as

$$V_r = \frac{W_{sb} G_{ss} \gamma_w}{W_{ss} G_{sb} \gamma_w} = \eta \frac{G_{ss} \gamma_w}{G_{sb} \gamma_w}, \tag{3}$$

where $W_{sb}(g)$ and $W_{ss}(g)$ are the weight of the biochar and soil solid, respectively; G_{sb} (-) and G_{ss} (-) are the specific gravity of biochar and soil, respectively, and γ_w (kN/m³) is the unit weight of water. η (%) is defined as biochar content in soil by mass ($\eta = \frac{W_{sb}}{W_{ss}}$). $V_r = 0$ means the void ratio of biochar-amended soil is equal to the void ratio of the bare soil (i.e., the pure soil without biochar). When V_r tends to be infinite, the void ratio of biochar-amended soil equals the void ratio of biochar. By knowing the e_i of biochar-soil composite, the saturated volumetric water content θ_s (%) can be expressed as

$$\theta_s = \frac{e_i}{1 + e_i}. \tag{4}$$

To take into account the influence of root decay on the SWRC, Ni et al. (2019) proposed a void ratio function that can model the decrease and increase of soil void ratio due to root occupancy upon growth and root shrinkage, respectively.

$$e = \frac{e_i - (1 - \xi)R_v(1 + e_i)}{1 + (1 - \xi)R_v(1 + e_i)}, \tag{5}$$

where e_i is the void ratio of biochar-amended soil, which is the sum of the microstructural void ratio (e_m) and the macrostructural void ratio (e_M), ξ (%) is the root decay rate. R_v (mm³/mm³) is the root volume ratio, which is defined as the total volume of roots per unit volume of soil. $R_v = 0$ means bare soil. R_v is less than $e_i/(1 + e_i)$, as total root volume cannot be larger than the total soil pore size. Depending on the plant type, R_v is a function of depth within the root zone.

The air entry value of biochar-amended vegetated soils considering root decay is expressed as follows:

$$\alpha = \frac{m_3}{e^{m_4}} \exp\left(-k \frac{e_r}{e_{r0}}\right), \tag{6}$$

where k (-) is a model parameter that controls the rate of reduction of the AEV due to root decay, and this parameter has to be dependent on the plant type and the soil media where it is grown; e_r (-) is the macro void ratio "returned" from root decay:

$$e_r = \frac{\xi R_v(1 + e_i)}{1 + (1 - \xi)R_v(1 + e_i)}, \tag{7}$$

and e_{r0} (-) is the void ratio occupied by roots (i.e., $e_0 - e$), when $\xi = 0$

By combining Eqs. (1)–(7), the influence of root growth and decay on soil water retention curves of biochar-amended vegetated coarse-grained soils can be expressed in Eq. (8).

$$S_r = \left[1 + \left(\frac{se^{m_4}}{m_3 \exp(-k \frac{e_r}{e_{r0}})} \left(\frac{C_m}{D_m} \eta + 1 \right)^{-m_5} \right)^{m_2} \right]^{-m_1}. \tag{8}$$

The widely used van Genuchten–Mualem–Fischer (VGM–Fischer) model (Fischer et al. 1996) assumed that the air permeability could be a function of the degree of water saturation S_r and maximum air permeability k_{a_max} (m²). VGM–Fischer model is expressed as

$$k_a = k_{a_max} (1 - S_r)^{0.5} (1 - S_r^m)^{2m}, \tag{9}$$

where m (-) is a fitting parameter depending on the pore size distribution, and k_{a_max} is the air permeability under completely dry conditions. Hence, by combing Eqs. (8) and (9), the gas permeability of biochar-amended unsaturated vegetated coarse-grained soils can be calculated. In the water retention and gas permeability model, there are three parameters for biochar properties (η , e_b and G_{sb}) and two for root properties (R_v , ξ).

2 Materials and methods

2.1 Validation of the water retention and gas permeability model

In order to validate the water retention and gas permeability model, a well-instrumented laboratory column test with biochar addition and grass transplantation was carried out. In addition, some relevant data from the literature were also selected, including Mei (2017), Ni et al. (2020) and Chen et al. (2020).

2.2 Soil, biochar and plant species

In the laboratory test, completely decomposed granite (CDG) was used. CDG is a common type of soil used in landfill covers in tropical and subtropical areas, such as Southern China (Ng et al. 2022b). The investigated soil

Table 1 Index properties of completely decomposed granite (CDG)

Index property	Value
Standard compaction tests	
Maximum dry density (kg m^{-3})	1870
Optimum moisture content (%)	12
Particle-size distribution	
Gravel content ($> 2 \text{ mm}$) (%)	19
Sand content ($\leq 2 \text{ mm}$) (%)	42
Silt content ($\leq 63 \mu\text{m}$) (%)	27
Clay content ($\leq 2 \mu\text{m}$) (%)	12
Specific gravity	2.60
Atterberg limits	
Plastic limit (%)	26
Liquid limit (%)	44
Plasticity index (%)	18
Unified Soil Classification System (USCS) ^a	Silty sand (SM)

^a ASTM (2010a)

contains 12% clay, 19% gravel, 27% silt and 42% sand. CDG was classified as silty sand, according to the Unified Soil Classification System (USCS, ASTM, 2010a). The optimum water content and maximum dry density are 12% and 1870 kg m^{-3} , respectively. The TOC and pH of this soil were determined to be $49.2 \pm 3.3 \text{ mg kg}^{-1}$ and 6.0 ± 0.01 , respectively. The soil contains 662 mg kg^{-1} of N and 363 mg kg^{-1} of P. Other properties of the CDG are listed in Table 1.

The biochar selected was pyrolyzed from the feedstock of peanut shell biomass. According to the obtained thermo-gravimetric analysis (TGA) of peanut shell biomass by Ni et al. (2020), the degraded mass decreases slowly when the heating temperature is lower than $400 \text{ }^\circ\text{C}$ and higher than $500 \text{ }^\circ\text{C}$. When the heating temperature increases from $400 \text{ }^\circ\text{C}$ to $500 \text{ }^\circ\text{C}$, the reduction in degraded mass is the most significant. The biochar in this study was produced at $400 \text{ }^\circ\text{C}$ with a residence time of 30–40 min under limited oxygen conditions. The properties of this type of biochar have been well-studied by Ni et al. (2018). The biochar was passed through a $425\text{-}\mu\text{m}$ sieve before mixing with CDG. The purpose was to achieve a more uniform biochar porosity and hence uniform soil–biochar composite, preventing any possible preferential flow during the test (Wong et al. 2017). It has been demonstrated that the small biochar particle size (smaller than $500 \mu\text{m}$) can enhance the positive effects of biochar application in sandy soils (Glab et al. 2016). Based on the Fourier-Transform Infrared Spectroscopy (FTIR) spectra of the biochar (Ni et al. 2020), there was a high peak spectral band at 3618 cm^{-1} named $-\text{OH}$ (hydrophilic) group. The spectral peak at 1708 cm^{-1} could

be due to the stretching vibration of $\text{C}=\text{O}$ bonds of the non-ionic carboxyl groups ($-\text{COOH}$, $-\text{COOCH}_3$). The peak at 1395 cm^{-1} was nominated to aromatic ($\text{C}=\text{C}-\text{C}$) vibrations. In addition, carbon (C) and oxygen (O) were dominant elements in the surface composition of the biochar. The specific area and true density of the biochar in this study were $8.45 \text{ m}^2\text{g}^{-1}$ and 1.96 g cm^{-3} , respectively. After sieving, the contents of biochar particles smaller than 0.002 mm , $0.002\text{--}0.02 \text{ mm}$ and larger than 0.02 mm were 32%, 41% and 27%, respectively. The pH of pure biochar was 7.5. The pH of the 10% biochar-CDG composite was 7.3, which is beneficial for the survival of *Cynodon dactylon* (Wong et al. 2019). More detailed description of the studied biochar is summarized in Table 2.

10% biochar (w/w) was mixed with CDG using a soil mixture. Those two materials were mixed continuously until the composite colour became uniform. Figure 1a shows the compaction curve of the CDG, and biochar-amended CDG. The maximum dry density for this biochar-CDG composite was 1740 kg m^{-3} , which was 8% smaller than that of bare CDG soil (Ni et al. 2018). With biochar addition, the optimum water content of CDG soil increased from 12% to 17%. 95% relative compaction was adopted in each column. Such relative compaction is commonly used to design slopes and landfill cover in the USA (TDOT 1981) and Hong Kong (GEO 2011). *Cynodon dactylon* can grow well under such high relative compaction (Ni et al. 2019). In order to reduce friction at the soil column interface, lubricant was applied on the inner surface of each column. A thin layer of geotextile was put at the bottom of each column to ensure uniform gas pressure distribution during the test. The composite was compacted in 16 layers in each column, spanning a height of 25 mm. Between each compacted layer, the soil surface was scarified to provide better contact and prevent preferential flow channels.

Table 2 Physico-chemical properties of the $425\text{-}\mu\text{m}$ sieved peanut shell biochar

Property	Value
Physico-chemical property	
Specific surface area (m^2g^{-1})	8.45
True density (g m^{-3})	1.96
pH	9.71 ± 0.04
Organic matter (%)	51.9 ± 0.09
Electric conductivity (ds m^{-1})	1.8 ± 0.09
Ash content (%)	48.09 ± 0.09
Particle size distribution	
$> 0.02 \text{ mm}$ (%)	0
$0.002\text{--}0.02 \text{ mm}$ (%)	72.1
$< 0.002 \text{ mm}$ (%)	27.9

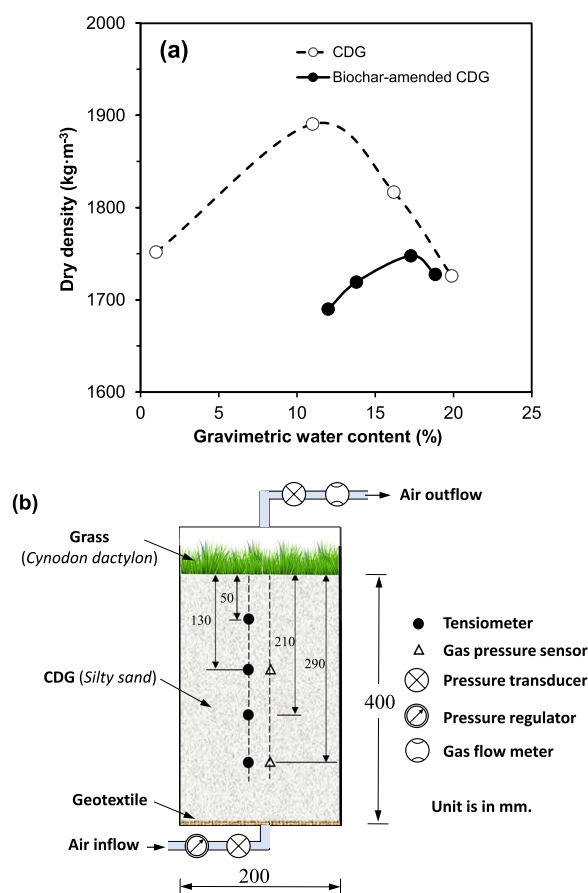


Fig. 1 a Influence of biochar on soil compaction curve and (b) test setup for the permeability test

After sample preparation in columns, a grass species *Cynodon dactylon* (also known as Bermuda grass) was transplanted. *Cynodon dactylon* was selected because it can provide ecological rehabilitation and restoration in landfill covers (GEO 2011). The grass turf with a root depth of 40 ± 8 mm and shoot length of 50 ± 6 mm was supplied by Tung Kee Garden Horticulture Ltd. in Hong Kong. The detailed transplantation procedures can refer to Ni et al. (2020). The grass was grown for two years in a well-controlled plant room. Irrigation was applied every three days during the growth period unless stated otherwise.

2.3 Test setup and instrumentation

There were eight columns in total, including three columns with grass, three biochar-amended columns with grass, one bare column and one biochar-amended column. Figure 1b shows the schematic diagram of each test column. As shown in Fig. 1, each column had a height of 400 mm and a diameter of 200 mm. The inner surface of all columns was filled with the self-solidifying silicon

glue to prevent any preferential gas flow through the gap between the soil and column. (Ng et al. 2015a). At the bottom of each column, there was a hole with a diameter of 5 mm to allow for free water drainage and gas influx during testing. All eight columns were placed in a well-controlled plant room. The relative humidity and air temperature were $60 \pm 5\%$ and 25 ± 1 °C, respectively. To facilitate plant growth, a constant radiant energy of 5.0 MJ m^{-2} was supplied on the top of all columns using cool fluorescent lamps (Ng et al. 2016a).

In order to measure the matric suction (i.e., negative pore water pressure) up to 90 kPa, an array of miniature-tip tensiometers (2100E, Soil Moisture Equipment Cooperation) were installed at depths of 50, 130, 210 and 290 mm in each column. Two gas pressure transducers (Chen 2016) were installed at 130 mm and 290 mm depths to measure gas pressure. Two types of airflow meters were used. The measuring ranges were $0\text{--}100 \text{ mL min}^{-1}$ and $0\text{--}30 \text{ L min}^{-1}$. The accuracies were 0.5 mL min^{-1} and 5 mL min^{-1} , respectively. It should be noted that a similar column setup was also used by Ni et al. (2020), who installed both miniature-tip tensiometers and soil moisture probes at the depths of 50, 130, 210 and 290 mm, but without gas pressure sensors. Since the testing conditions (soil and biochar type, grass turf, growth duration and atmospheric parameters) between this study and Ni et al. (2020) are the same, the measured soil water retention curves by Ni et al. (2020) were also used in this study.

2.4 Testing procedures

After grass growth for 24 months, gas permeability was measured for all eight columns. Before each gas permeability test, all columns were saturated by applying water ponding on the top. Water ponding stopped when basal water percolation occurred, and suction readings at all depths became zero. All the columns were left for drying in the plant room. At random suction distribution during the drying period, a gas permeability test was carried out. The procedures can follow Ni and Ng (2019). The applied gas was carbon dioxide, and the adopted gas pressure at the bottom of each column was 20 kPa, based on the suggestion by Chen (2016). 20 kPa can represent the worst scenario of bottom gas pressure in the in-situ landfill cover. A gas flow meter was installed on the top to measure the gas flow rate after the breakthrough. Gas pressures at 130 mm and 290 mm depths were also recorded during the gas permeability test. Finally, Darcy's law was used to calculate the gas flow velocity.

Before the continuous gas emission test, all the saturated columns were subjected to evaporation or evapotranspiration in the plant room until the suction at the shallow depth (i.e., 50 mm) reached ~ 60 kPa. The gas

emission test lasted for ten days, during which gas pressure distribution along depth and gas emission rate at the top were recorded on Days 2, 5 and 8. During the test, all the ambient atmospheric parameters were kept constant to minimize the disturbance to the gas emission test. After the gas permeability test, soil cores 76 mm in diameter and 100 mm in height were sampled from 0 and 100 mm depths in each column using a cylindrical core cutter. Three replicated cores were collected from vegetated columns. In total, there were eight core samples tested. The saturated permeability of each core sample was then measured using the falling head method according to ASTM (2010b) standard D5084. The detailed testing procedures can refer to Ni et al. (2017). Finally, saturated permeability values of 8 core samples were calculated using Darcy’s law. After the water permeability test, all soil core samples from the shallow depths of each column were carefully washed, and roots were analyzed to determine the root volume ratio (R_v). Detailed measurement procedures can be found in Ni et al. (2019). By excavating the soils in each column, root depth was also measured.

In order to highlight the effects of grass and biochar on measured field capacity (FC), permanent wilting point (PWP) and gas permeability, one-way ANOVA analysis was adopted. In the analysis, significant differences were assessed, followed by post hoc Fisher’s least-significant-difference test. Results were considered statistically significant when p -value < 0.05. Different letters (a, b, c, d) were used to indicate the statistical significance of differences among groups.

2.5 Numerical plan, model setup and procedures

In order to investigate the significance of biochar and plant growth on gas emission in conventional one-layer landfill covers, a series of numerical analyses were carried out using commercial software Air/W (Geostudio). The numerical study was composed of two stages. In the first stage, the laboratory column test results from this study were used to calibrate the numerical model setup. In the second stage, parametric studies were conducted using the calibrated numerical model setup to further explore the influences of root depth and extreme drought conditions on gas emission rate.

In the first stage, a one-dimensional model was established according to the configuration of the soil column test. The soil thickness was 0.4 m, and the initial depth of the grass root zone was 0.2 m, based on the measured results. For simplicity, root distribution was assumed to be in a uniform pattern. A uniform mesh configuration for 1D geometry was adopted. A total number of 800 rectangular elements were generated in the mesh configuration to simulate the soil column. Regarding the hydraulic

boundary conditions, the top surface was set to a zero-flux boundary, and the bottom end was set as a unit-gradient flux boundary for free water drainage. Zero water flux was specified as the side boundaries. For the gas flow boundary, a zero-gas pressure was applied at the top, while a constant gas pressure of 20 kPa was applied at the base of each column. Zero gas flux was specified as the side boundary conditions. The calculated water retention curves and gas permeability functions using the new theoretical model were input for each soil domain in the numerical model. The required unsaturated permeability functions of the materials were calculated from their corresponding water retention curves in Fig. 2a based on the van Genuchten–Mualem equation (van Genuchten 1980; Mualem 1976). The saturated water permeability of bare, grass, biochar and grass + biochar cases after 24 months of grass growth were determined to be 4.26×10^{-6} m

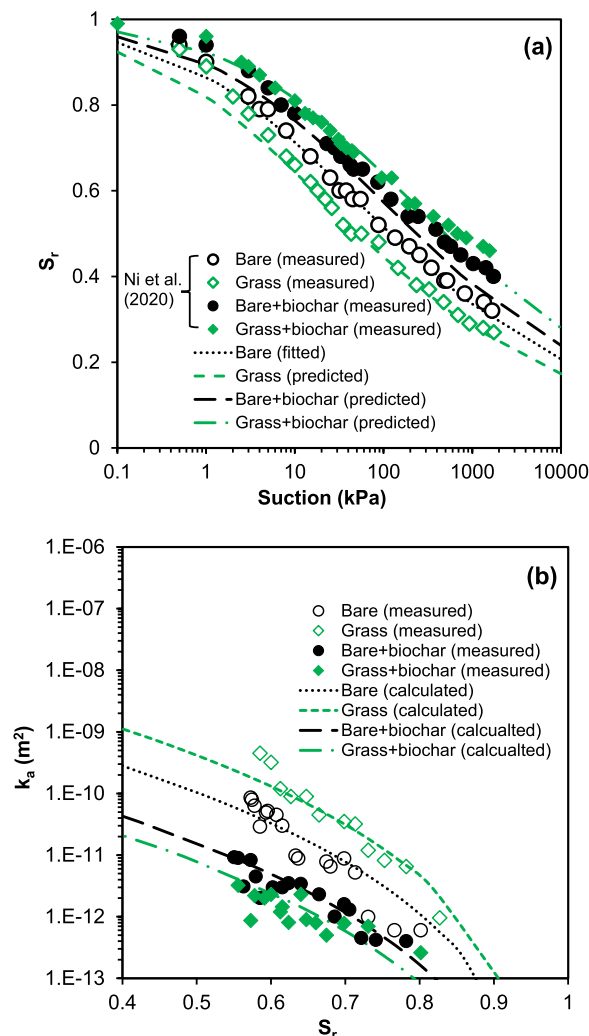


Fig. 2 Comparison between the measured and calculated (a) water retention curves and (b) gas permeability function

Table 3 Summary of parameters for the new water retention model and gas permeability model

From	Test ID	Parameters for the new SWRC models										Biochar properties			Root properties		Parameters for gas flow	
		e_s (-)	G_{ss} (-)	m_1 (-)	m_2 (-)	m_3 (kPa)	m_4 (-)	m_5 (-)	η (%)	e_b (-)	G_{sb} (-)	R_v (mm ³ mm ⁻³)	ξ (%)	$k_{a,max}$ (m ²)	m (-)			
Ni and Ng (2019)	Bare	0.65	2.63	0.49	0.46	1.5	4.4	20	0	1.5	1.43	-	-	2e-8	2.0			
	Grass								0		0.046	17		8e-8				
This study	Bare + biochar								10					3e-9				
	Grass + biochar								10		0.069	6		1.5e-9				
Mei (2017)	Bare	0.77	2.60	0.07	2.5	0.8	5.7	20	0	-	-	0		1e-6	0.8			
	Grass1										0.0032			5e-7				
	Grass2										0.012			2e-7				
Chen et al. (2020)	Grass3										0.018			8e-8				
	Bare	0.98	2.62	0.25	1.1	18	3.6	20	0	1.8	2.07	-		3e-6	0.8			
	Bare + biochar								10					1e-6				

e_s (-) is the void ratio of bare soil; G_{ss} (-) is the specific gravity of soil; m_1, m_2, m_3, m_4 are the mode parameters; m_1 (-) and m_2 (-) determine the shape of a SWRC; m_3 (kPa) and m_4 (-) are related to the air-entry value (AEV) of the soil; m_5 (-) is a soil parameter for describing the effects of pore structure on AEV; η (%) is the biochar ratio; R_v (mm³mm⁻³) is the plant root volume ratio and a function of depth within the root zone; e_b (-) is the void ratio of pure biochar; G_{sb} (-) is the specific gravity of biochar; ξ (%) is the root decay rate; $k_{a,max}$ (m²) is the air permeability under completely dry conditions; m (-) is a fitting parameter depending on the pore size distribution. k is determined to be 10, according to Ni et al. (2019); m_5 and D_m are adopted based on Ng et al. (2022a); C_{m1} is back-calculated to be 0.28 based on the test results in this study

s^{-1} , $1.23 \times 10^{-5} \text{ m s}^{-1}$, $5.47 \times 10^{-7} \text{ m s}^{-1}$ and $1.74 \times 10^{-7} \text{ m s}^{-1}$, respectively. The average R_v values within the shallow depth of 100 mm were measured to be 0.046 and 0.069 $\text{mm}^3 \text{mm}^{-3}$ in the grass and grass + biochar cases, respectively. The root depths after 24 months of growth were about 0.2 m in both cases. For the grass column or grass + biochar column, the domains within the root zone (top 0.2 m) and below the root zone should be specified with different soil hydraulic properties and gas permeability functions. Before the gas emission simulation, the initial suction distribution in each column was set based on the measured results. Gas emission simulation last for ten days, during which evaporation and evapotranspiration were not simulated.

In the second stage, two series of parametric analyses were carried out. The first series focused on the effects of root depth on the gas emission rate. Apart from the 0.2 m root depth in the model calibration run, another root depth of 0.4 m was considered in the analysis. For simplicity, soil hydraulic properties and gas permeability functions in the original top 0.2 m root zone were copied to the bottom 0.2 m for both grass and grass + biochar cases. Uniform root distribution was specified along the entire soil domain. The second series aimed to study the extreme drought on the gas emission in four soil conditions. A high initial suction of 500 kPa was specified for all the soil columns to represent the extremely dry scenario. The calculated gas emission rate from this high suction condition was compared against that in the model calibration run in the first stage. The boundary conditions and other testing procedures were exactly the same as those in the first stage of numerical analysis.

3 Results and discussion

3.1 Interpretations of test results

Figure 2a shows the comparison between the measured and calculated water retention curves under four conditions (i.e., bare, grass, bare + biochar and grass + biochar). All the measured data were from Ni et al. (2020). By fitting the SWRC of bare soil, the parameters m_1 , m_2 , m_3 and m_4 (see Table 3) were calibrated. The parameters m_5 and D_m were selected based on the suggestions by Ng et al. (2022a). The parameter for biochar effects on soil microstructure was back-calculated to be 0.28. Based on the calibrated parameters in Table 3, the SWRCs of grass, bare + biochar and grass + biochar were calculated. Good matches were found for all three cases, with a maximum discrepancy of less than 14%. It can be seen that after 24-month growth, grassed soil has a relatively smaller water retention capacity than bare soil. S_r values at field capacity (FC) and permanent wilting point (PWP) for the grass case were statistically larger than those of the bare case, respectively, with a p -value less than 0.05

(Table 4). However, for biochar-amended soil or grassed soil, the water retention capacity was consistently higher than that of the bare soil over the wide range of suction (0–1100 kPa). The water-holding capacity was the most significant when biochar and grass were present. The significant differences (p -value < 0.05) among the four cases (i.e., bare, grass, bare + biochar and grass + biochar) in terms of S_r values at FC and PWP have been demonstrated by the one-way statistical analysis (Table 4). This is because biochar has stable chemical and physical properties (Burrell et al. 2016). Biochar has a porous structure, which behaves as additional capillary tubes with smaller pore throats, favouring additional water storage in soils (Blanco-Canqui 2017). In addition, the biochar produced from peanut shells has high polarity and an abundance of O-containing functional groups, enhancing the water adsorption capacity (Jing et al. 2018). Biochar can beneficially promote the growth of plants by increasing water retention capacity and providing nutrients. Even though there might be a small number of decayed roots in grassed soil with biochar amendment, the promoted growth of healthy roots by biochar can occupy more soil pores, outweighing the negative effects of decay roots induced macropores. Both the model and test results indicate that biochar can enhance soil water retention capacity due to its unique micropore structure and promotion of plant growth.

Figure 2b compares measured and calculated gas permeability under various degrees of saturation. This relationship is also called the gas permeability function. Gas permeability values under four ground conditions (i.e., bare, grass, bare + biochar, grass + biochar) are presented. The maximum air permeability was back-calculated based on the measured data, and the fitting parameter was calibrated to be 2.0. Generally, gas permeability (k_g) decreased nonlinearly with the increase in the degree of saturation (S_r). When the S_r was larger than 0.8, the reduction of gas permeability became much faster. This is because at higher S_r , air pores in soils are much less connected and hence fewer channels are available for airflow. It shows clearly that at any given S_r , the k_g of the grass case was larger than that of the bare case by about four times. At $S_r=0.6$, the significant differences in k_g between the grass and bare cases are shown in Table 4 (indicated by the letters). However, compared with the bare case, the biochar-amended soil and grassed soil had smaller k_g by up to 2 times of magnitude, depending on the S_r . The reduction of average k_g in the grass + biochar case was the most substantial. However, based on the statistical analysis for the k_g results at $S_r=0.6$, the difference between the biochar case and grass + biochar case was not significant (p -value > 0.05), while the grass case and bare case were significantly larger than both the

Table 4 Variations of the degrees of saturations (S_r) at field capacity (FC), permanent wilting point (PWP) and gas permeability (k_g) at $S_r=0.6$ (mean \pm standard error of mean)

Test case	S_r at FC (-)	S_r at PWP (-)	k_g at $S_r=0.6$ (m^2)
Bare	$0.55 \pm 0.03b$	$0.30 \pm 0.02b$	$(3.4 \pm 0.9) \times 10^{-11}b$
Grass	$0.47 \pm 0.03a$	$0.24 \pm 0.03a$	$(1.6 \pm 1.1) \times 10^{-10}c$
Biochar	$0.76 \pm 0.04c$	$0.43 \pm 0.03c$	$(5.4 \pm 1.0) \times 10^{-12}a$
Grass + Biochar	$0.85 \pm 0.03d$	$0.51 \pm 0.02d$	$(2.3 \pm 1.1) \times 10^{-12}a$
<i>p</i> -value	<0.001	<0.001	0.067

bare and grass cases. Biochar-induced decrease in k_g was also observed by Villagra-Mendoza and Horn (2018) in a sandy loam amended with mango-wood biochar and Garg et al. (2019) using water-hyacinth biochar particles. Even though adding biochar can slightly increase the average pore void ratio, the measured gas permeability in biochar-amended soil decreased. This is because the additional water in the intra-pores of biochar reduces the air conductive channels for gas migration, resulting in a decrease in k_g of biochar-amended soils. On the other hand, the increase in biochar addition could increase the possibility of pore-clogging and tortuosity in soil (Githinji 2014) and hence offset the increase of saturated water permeability due to the increased average void ratio. Besides, biochar can decrease the number of desiccation cracks by at least 50% compared to bare soil (Bordoloi et al. 2018). This can be another reason that causes the reduction of gas permeability in biochar-amended soils. When considering the plant root-biochar interactions, the promoted plant root can further occupy the inter- and intra-pore voids of biochar, hence reducing the available channels for gas migration.

Figure 3 shows the comparison between measured and calculated gas permeability function in four soils vegetated with Vetiver grass. Gas permeability values under four conditions ($R_v=0, 0.0032, 0.012$ and $0.018 \text{ cm}^3\text{cm}^{-3}$) were measured in the laboratory (Mei 2017). There was no biochar addition in this test ($\eta=0$). No root decay was observed. Under each vegetated soil, four soil water contents were considered. The overall trend between k_g and S_r was similar to that in Fig. 2b. The gas permeability model can almost capture the variations of k_g with S_r and R_v . The presence of young roots can decrease gas permeability at any water content. The decreased amount of k_g is due to plant roots becoming smaller under higher S_r . This is because plant roots occupy soil pore space and decrease the flow channels for gas migration. In order to further demonstrate the feasibility of the proposed model, another dataset from Chen et al. (2020) was selected, as shown in Fig. 4. In Chen et al. (2020), the

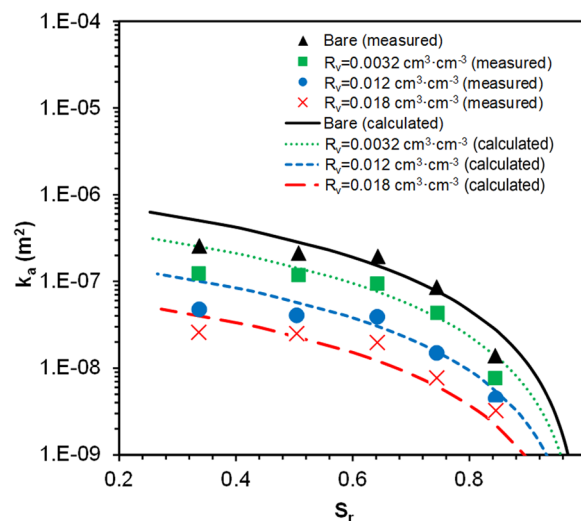


Fig. 3 Comparison between the measured (Mei 2017) and calculated gas permeability function

soil was amended with peanut shell biochar but without the transplantation of vegetation ($R_v=0$). k_g decreased gradually with the increase of S_r . The presence of biochar particles decreased the k_g at the same magnitude when S_r varies from 0.1 to 0.4 due to the clogging of soil pores by biochar particles. The gas permeability model can capture the variations of k_g with S_r . All the results from Figs. 2, 3, 4 demonstrate the practical feasibility of the model.

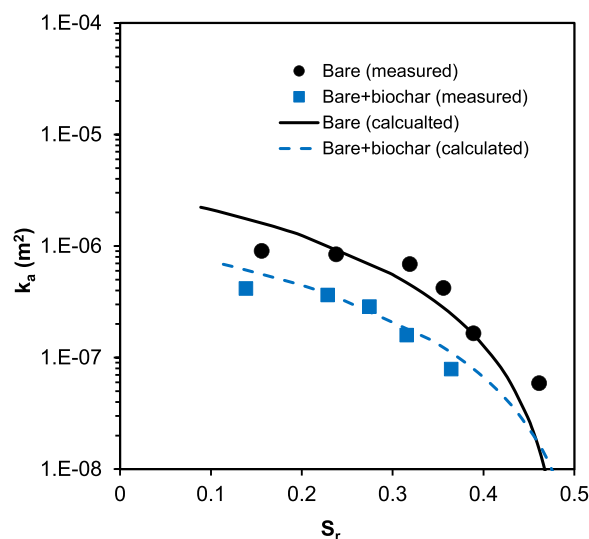


Fig. 4 Comparison between the measured (Chen et al. 2020) and calculated gas permeability function

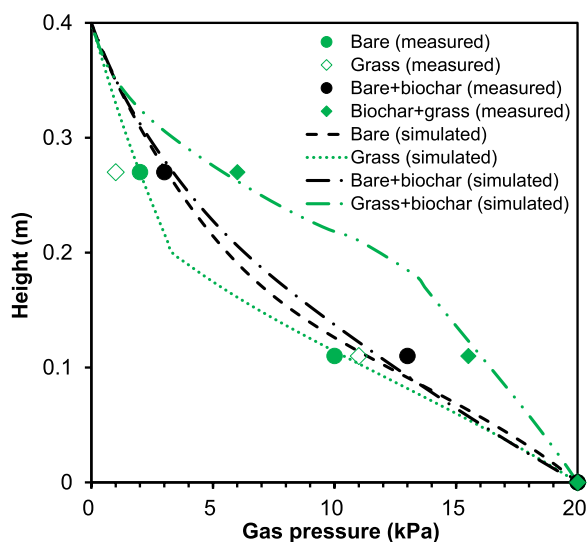


Fig. 5 Comparison between the measured and simulated gas pressure distribution along soil column

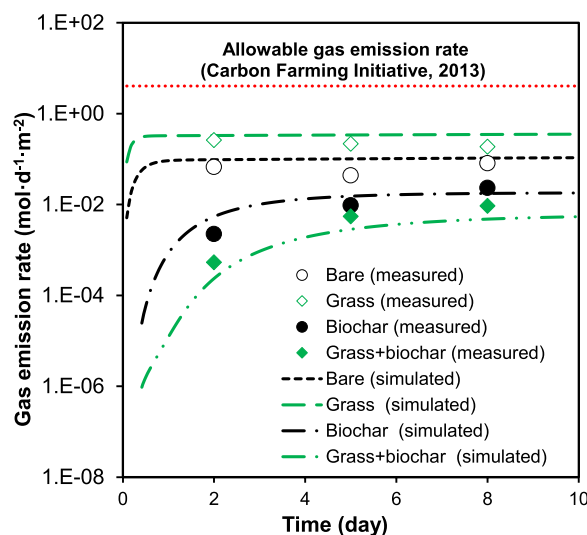


Fig. 6 Comparison between the measured and simulated gas emission rate in each soil column

3.2 The significance of biochar and vegetation on gas emission in landfill covers

3.2.1 Calibration of the numerical model

Figure 5 compares the simulated and measured gas pressure distribution along depth in the validation. Gas pressure increased from 0 to 20 kPa along the depth. The gas pressure gradient at the shallow depth (150 mm) was much smaller than that at the deeper depth (below 300 mm) for the bare, biochar and grass cases. However, the gas pressure gradient at shallow depths in the grassed column was much smaller than that of bare and biochar cases. In the grassed column, the observed decay roots at shallow depths can become preferential flow channels (Ni et al. 2020) for gas migration. Hence, less energy is required to transport the gas from the middle to the top of the column. However, compared with the bare and biochar cases, the grass + biochar case had a larger pressure gradient at the shallow depth. According to the result in Fig. 2b, the grass + biochar case had the smallest gas permeability among the four cases when plant roots and biochar coexisted within the top 200 mm of the column. Therefore, a larger gas pressure gradient is required at the shallow depth under a given gas flow rate. At the deeper depth between 200 and 400 mm, it became the opposite that the grass case had the largest gas pressure gradient, followed by bare or biochar cases and then the grass + biochar case. By comparing the computed and measured results, the established numerical model can capture gas pressure distributions in vegetated soils with biochar addition quite well, except for the bare case. This is likely because the observed tiny cracks in the

bare column are not taken into account in the numerical simulation.

Figure 6 compares the measured and simulated gas emission rates in all four types of soil columns. The allowable gas emission rate required by design guideline (CFI 2013) is also superimposed to interpret the results. The comparison demonstrates that the numerical model can reasonably capture the variations of gas emission rate with time when vegetation and biochar are present. Overall, the gas emission rates in different columns increase rapidly with time and then approach the steady state. A similar pattern was also reported by Ng et al. (2015b) and Feng and Liu (2022). It took about half a day for bare and grass cases, while it took about six days for grass + biochar cases to reach a constant gas emission rate. At the steady state (Day 10), the gas emission rate in the grass case was about two orders of magnitude higher than that in the grass + biochar case. This difference is consistent with the gas permeability results in Fig. 2b. The presence of biochar with small particles increases the possibility of pore-clogging and tortuosity in soil (Githinji 2014). Hence, it takes more time for gas to fully breakthrough the soil column. However, it should be noted that when coarse biochar with particle size > 0.425 mm is mixed in the soil, the amount of macropores and pore connectivity in the soil might increase, and it is easier for gas to migrate through the soil (Chen et al. 2020). The gas emission rates in all four cases are at least one order of magnitude smaller than the allowable value in the design guideline (CFI 2013). The results imply that the landfill cover can perform well when soil suction is not higher than 60 kPa, even though biochar is not added.

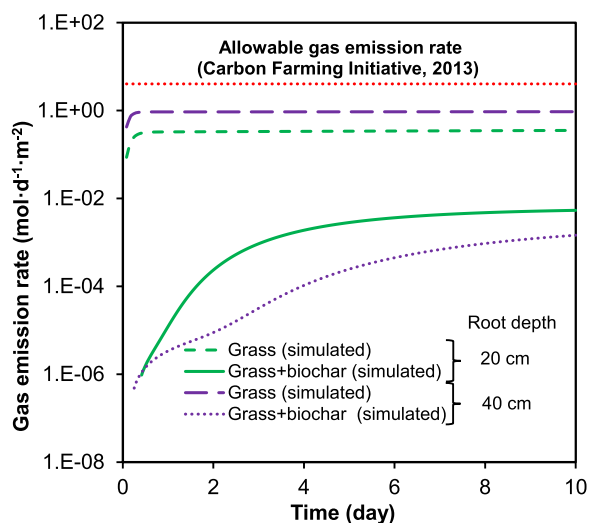


Fig. 7 Influence of root depth on gas emission

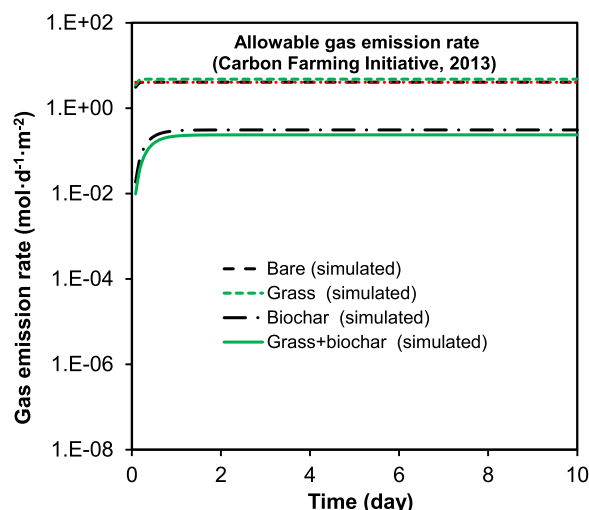


Fig. 8 Simulated gas emission rate at extremely dry conditions (suction around 500 kPa)

3.2.2 Influence of root depth and extreme drought on gas emission rate

Figure 7 shows the influence of root depth on gas emission rate when the surface suction is about 60 kPa. Only grass and grass+biochar cases are presented. When root depth increased from 0.2 m to 0.4 m, the steady-state gas emission rate in only the grass case increased by about 170%. This is because when grass root depth extends from 0.2 m to 0.4 m, the bottom half of the column changes from bare soil to grass soil. The gas permeability of grass soil is always larger than that of bare soil at any given degree of saturation (Fig. 2b). Hence, gas migration becomes easier when the root depth is 0.4 m, resulting in a higher gas emission rate. Even though the deeper root depth (i.e., from 0.2 m to 0.4 m) can cause an increase in gas emission rate, it is still below the allowable gas emission rate required by design guideline (CFI 2013). Caution should be taken that the allowable gas emission rate can be exceeded when the further growth of roots (i.e., higher root length density) and more decay roots are observed. However, for the grass+biochar case, the gas emission rate at the root depth of 0.4 m was up to 97% smaller than that at the root depth of 0.2 m. When the bottom half of the column changes from biochar soil to grass+biochar soil, its corresponding gas permeability function shifts downwards, as shown in Fig. 2b. The reduced gas permeability at any degree of saturation causes the reduction in gas migration and hence lower gas emission rate in the grass-biochar case. The results in Fig. 7 imply that in order to minimize the negative influence of root growth (i.e., deeper root depth) on the gas emission in landfill cover, biochar is highly

recommended to be mixed in soils to promote the positive contribution from grass.

Figure 8 shows the effects of extreme drought on gas emission rate in four column conditions. A high suction of 500 kPa was assumed in each column to represent the extreme condition. The gas emission rate increased during the initial half day and then became constant until ten days. Compared with the low suction condition (60 kPa) in Fig. 6, at higher suction (500 kPa), a shorter time was required to stabilize the gas emission rate, and the steady-state value was larger by at least 12.5 times. Among the four soil conditions, gas emission rates in bare and grass cases were very close, which was at least one order of magnitude larger than that in biochar and grass+biochar cases. According to the water retention curves in Fig. 2a, retained water in soil reduces significantly at high suction conditions, including the water in inter- and intra-biochar pores in biochar particles. Hence, a high suction leads to a high air permeability (Fig. 2b), and more available connected pore channels can facilitate the gas migration under a pressure gradient. Ng et al. (2015b) reported that after drying for 34 days, the single-clay layer and conventional capillary barrier landfill covers could not effectively act as a gas barrier due to the rapid increase of gas permeability under high suction. In this study, the final steady-state gas emission rate in the grass case was 18% larger than the allowable value stated in the guideline (CFI 2013). The bare case reached the same gas emission rate as the allowable value. However, with the presence of biochar, the gas emission rate was still much lower than the allowable value. This is because, in the biochar or grass+biochar case, the degree of saturation at the suction of 500 kPa was 15–50% larger than

those in bare and grass cases (Fig. 2a). Hence, a much smaller gas permeability resulted, according to Fig. 2b. It should be noted that in the simulated drought condition, drying-induced soil cracks were not considered in the simulation. Several researchers have studied gas migration in cracked fine-grained soil, such as clay. Zettwoog et al. (1982) measured the gas flux density from cracked and uncracked surfaces and quoted an order of magnitude change. Rogers et al. (1984) investigated the effect of cracks on surface gas emission and observed that 4% of an area opened by cracks could halve the effective thickness of a tailing cover. Commonly, desiccation cracks occur when the drying shrinkage is constrained and the soil tensile strength is reached (Roy and Rajesh 2023). However, desiccation cracks were rarely found in the coarse-grained soils as the coarse-grained particles can reduce soil shrinkage (Zhao and Santamarina 2020). Therefore, the soil cracking induced by desiccation on the gas emission through the coarse-grained soil would be insignificant. It has also been reported that biochar addition can minimize the propagation of soil cracks (Zhang et al. 2020; Yang et al. 2021). The results in Fig. 8 indicate that when designing the earthen landfill cover, the most unsafe condition (grass or bare case at high suction) should be avoided. Instead, the approach of using both biochar amendment and vegetation can be adapted to retain relatively higher water content and lower gas permeability.

4 Conclusions

This study developed a new and simple gas permeability model for vegetated coarse-grained soil with biochar. A laboratory soil column test and two tests from the literature were used to validate the gas permeability model and calculated gas emission rate. Based on the validated model, a series of numerical analyses were carried out to investigate the influence of root depth and extreme soil drought on gas emission rate. The result was interpreted together with the design guideline. Finally, some design recommendations were provided for researchers and engineers. The key conclusions are summarized as follows:

1. The newly developed gas permeability required five parameters for peanut shell biochar and Bermuda grass. By comparing the measured and calculated results, the model was demonstrated to satisfactorily capture the influence of biochar particles and plant roots on gas migration in unsaturated landfill cover.
2. Among the four soil conditions (bare, grass, biochar and grass + biochar), the grass case had the highest gas emission rate, followed by bare, biochar and grass + biochar cases. The largest difference can be up

to two orders of magnitude. This is because grassed soil with decayed roots has the largest gas permeability at any water content. On the contrary, peanut shell biochar- Bermuda grass interaction reduces the root decay rate and retains the highest water retention capacity and the lowest gas permeability.

3. With the further growth of Bermuda grass roots (i.e., deeper root depth), gas emission increased obviously in grass and grass + biochar cases. When the soil suction increased to 500 kPa (extreme dry condition), the gas emission rate in the grass case further increased, and its steady-state value was larger than that in the design guideline, indicating the failure of grassed cover acting as a gas barrier. However, the gas emission rate in the grass + biochar case was still lower than the value in the design guideline.
4. To promote the effectiveness of vegetated landfill cover in reducing gas emissions, it is highly recommended to use peanut shell biochar (e.g., 10%) as a soil amendment to promote the performance of Bermuda grass in maintaining high water retention and low gas emission even under drought conditions.

Acknowledgements

The authors would like to thank the support of the Fundamental Research Funds for the Central Universities (Grant No. 3221002220A1) and the State Key Laboratory of Subtropical Building Science in South China University of Technology (Grant No. 2022ZC01).

Author contributions

JN: Conceptualisation, Methodology, Investigation, Writing—original draft, Project administration; JZ: Investigation, Data curation, Writing—review and editing; YW: Methodology, Data curation, Writing—review and editing, Formal analysis; HG: Conceptualisation, Methodology, Investigation, Writing—original draft.

Funding

This work was financially supported by the Fundamental Research Funds for the Central Universities (Grant No. 3221002220A1) and the State Key Laboratory of Subtropical Building Science in South China University of Technology (Grant No. 2022ZC01).

Availability of data and materials

The datasets used or analyzed during the current study are available from the corresponding author on reasonable request.

Declarations

Competing interests

The authors declare that they have no known competing financial interests or personal relationships that could have appeared to influence the work reported in this paper.

Author details

¹School of Transportation, Southeast University, Nanjing, China. ²Department of Civil and Environmental Engineering, The Hong Kong University of Science and Technology, Hong Kong SAR, China.

Received: 21 February 2023 Revised: 9 July 2023 Accepted: 13 July 2023
Published online: 03 August 2023

References

- ASTM (2010a) Standard practice for classification of soils for engineering purposes (Unified Soil Classification System). ASTM standard D2487. American Society for Testing and Materials, West Conshohocken, Pa. <https://doi.org/10.1520/D2487-11>.
- ASTM (2010b) Standard test methods for measurement of hydraulic conductivity of saturated porous materials using a flexible wall permeameter. ASTM standard D5084. West Conshohocken, Pa. doi:<https://doi.org/10.1520/D5084-00>.
- Blanco-Canqui H (2017) Biochar and soil physical properties. *Soil Sci Soc Am J* 81:687–711
- Bordoloi S, Garg A, Sreedeeep S, Lin P, Mei GX (2018) Investigation of cracking and water availability of soil–biochar composite synthesized from invasive weed water hyacinth. *Bioresour Technol* 263:665–677
- Burrell LD, Zehetner F, Rampazzo N, Wimmer B, Soja G (2016) Long-term effects of biochar on soil physical properties. *Geoderma* 282:96–102
- Carbon Farming Initiative (CFI) (2013) Guidelines for calculating regulatory baselines for legacy waste landfill methane projects. Canberra, Australia: Australian Government.
- Chen ZK (2016) Gas Breakthrough and Emission in Unsaturated Landfill Final Cover Considering Cracking Effect. PhD Thesis. The Hong Kong University of Science and Technology, Hong Kong.
- Chen Z, Chen C, Kamchoom V, Chen R (2020) Gas permeability and water retention of a repacked silty sand amended with different particle sizes of peanut shell biochar. *Soil Sci Soc Am J* 84(5):1630–1641
- Feng S, Liu HW (2022) Numerical study of landfill gas emissions through three earthen landfill covers. *J Environ Eng-ASCE* 148(8):04022041
- Fischer U, Schulin R, Keller M (1996) Experimental and numerical investigation of soil vapor extraction. *Water Resour Res* 32:3413–3427
- Gallipoli D, Wheeler SJ, Karstunen M (2003) Modelling the variation of degree of saturation in a deformable unsaturated soil. *Géotechnique* 53(1):105–112
- Garg A, Bordoloi S, Ni JJ, Cai WL, Maddibiona PG, Mei GX, Poulsen TG (2019) Influence of biochar addition on gas permeability in unsaturated soil. *Geotech Lett* 9(1):66–71
- Garg A, Huang H, Cai W, Reddy NG, Chen P, Han Y, Zhu HH (2021) Influence of soil density on gas permeability and water retention in soils amended with in-house produced biochar. *J Rock Mech Geotech* 13(3):593–602
- GEO (Geotechnical Engineering Office) (2011) Technical Guidelines on Landscape Treatment for Slopes. Geotechnical Engineering Office, Hong Kong, China.
- Ghestem M, Sidle RC, Stokes A (2011) The influence of plant root systems on subsurface flow: implications for slope stability. *Bioscience* 61(11):869–879
- Githinji L (2014) Effect of biochar application rate on soil physical and hydraulic properties of a sandy loam. *Arch Agron Soil Sci* 60:457–470
- Glab T, Palmowska J, Zaleski T, Gondok K (2016) Effect of biochar application on soil hydrological properties and physical quality of sandy soil. *Geoderma* 281:11–20
- Grzesiak S, Grzesiak MT, Filek W, Hura T, Stabryła J (2002) The impact of different soil moisture and soil compaction on the growth of triticale root system. *Acta Physiol Plant* 24(3):331–342
- Guo HW, Zhang Q, Chen YB, Lu H (2023) Effects of biochar on plant growth and hydro-chemical properties of recycled concrete aggregate. *Sci Total Environ* 882:163557
- Hamamoto S, Moldrup P, Kawamoto K, Wickramarachchi PN, Nagamori M, Komatsu T (2011) Extreme compaction effects on gas transport parameters and estimated climate gas exchange for a landfill final cover soil. *J Geotech Geoenviron-ASCE* 137(7):653–662
- Hossain MZ, Bahar MM, Sarkar B, Donne SW, Ok YS, Palansooriya KN, Kirkham MB, Chowdhury S, Bolan N (2020) Biochar and its importance on nutrient dynamics in soil and plant. *Biochar* 2:379–420
- Jing F, Sohi SP, Liu Y, Chen J (2018) Insight into mechanism of aged biochar for adsorption of PAEs: reciprocal effects of ageing and coexisting Cd²⁺. *Environ Pollut* 242:1098–1107
- Kobayashi A, Takahashi A, Kakimoto Y, Miyazawa Y, Fujii N, Higashitani A, Takahashi H (2007) A gene essential for hydrotropism in roots. *Proc Natl Acad Sci USA* 104(11):4724–4729
- Kumar H, Ganesan SP, Bordoloi S, Sreedeeep S, Lin P, Mei GX, Garg A, Sarmah AK (2019) Erodibility assessment of compacted biochar amended soil for geoenvironmental applications. *Sci Total Environ* 672:698–707
- Kumar A, Bhattacharya T, Mukherjee S, Sarkar B (2022) A perspective on biochar for repairing damages in the soil–plant system caused by climate change-driven extreme weather events. *Biochar* 4(1):22
- Lehmann J, Joseph S (2009) Biochar for environmental management: science and technology. *Earthscan* 25(1):15801–15811
- Maeght JL, Gonkhamdee S, Clément C, Isarangkool Na Ayutthaya S, Stokes A, Pierret A (2015) Seasonal patterns of fine root production and turnover in a mature rubber tree (*Hevea brasiliensis* Müll. Arg.) stand—differentiation with soil depth and implications for soil carbon stocks. *Funct Plant Ecol* 6:1022
- Major J, Lehmann J, Rondon M, Goodale C (2010) Fate of soil-applied black carbon: downward migration, leaching and soil respiration. *Glob Change Biol* 16(4):1366–1379
- Mei Z (2017) Experimental study on the temperature effects on water and gas permeability of unsaturated rooted soils. Shenzhen Graduate School, Harbin Institute of Technology, MPhil Thesis (in Chinese).
- Moore F, González ME, Khan N, Curaqueo G, Sanchez-Monedero M, Rilling J, Morales E, Panichini M, Mutis A, Jorquera M, Mejias J (2018) Copper immobilization by biochar and microbial community abundance in metal-contaminated soils. *Sci Total Environ* 616:960–969
- Mualem Y (1976) A new model for predicting the hydraulic conductivity of unsaturated porous media. *Water Resour Res* 12(3):513–522
- Nan Q, Xin L, Qin Y, Waqas M, Wu W (2021) Exploring long-term effects of biochar on mitigating methane emissions from paddy soil: a review. *Biochar* 3(2):125–134
- Ng CWW, Chen ZK, Coo JL, Chen R, Zhou C (2015) Gas breakthrough and emission through unsaturated compacted clay in landfill final cover. *Waste Manage* 44:155–163
- Ng CWW, Ni JJ, Leung AK, Zhou C, Wang ZJ (2016a) Effects of planting density on tree growth and induced soil suction. *Géotechnique* 66(9):711–724
- Ng CWW, Coo JL, Chen ZK, Chen R (2016b) Water infiltration into a new three-layer landfill cover system. *J Environ Eng-ASCE* 142(5):04016007
- Ng CWW, Guo H, Ni J, Zhang Q, Chen ZK (2022a) Effects of soil–plant–biochar interactions on water retention and slope stability under various rainfall patterns. *Landslides* 19(6):1379–1390
- Ng CWW, Guo HW, Ni JJ, Chen R, Xue Q, Zhang YM, Feng Y, Chen ZK, Feng S, Zhang Q (2022b) Long-term field performance of non-vegetated and vegetated three-layer landfill cover systems using construction waste without geomembrane. *Géotechnique*. <https://doi.org/10.1680/jgeot.21.00238>
- Ng CWW, Liu J, Chen R (2015b) Numerical investigation on gas emission from three landfill soil covers under dry weather conditions. *Vadose Zone J* 14(8).
- Nguyen TKL, Ngo HH, Guo W, Chang SW, Nguyen DD, Nghiem LD, Hai FI (2019) Insight into greenhouse gases emissions from the two popular treatment technologies in municipal wastewater treatment processes. *Sci Total Environ* 671:1302–1313
- Ni JJ, Ng CWW (2019) Long-term effects of grass roots on gas permeability in unsaturated simulated landfill covers. *Sci Total Environ* 666:680–684
- Ni JJ, Leung AK, Ng CWW, So PS (2017) Investigation of plant growth and transpiration-induced matric suction under mixed grass–tree conditions. *Can Geotech J* 54(4):561–573
- Ni JJ, Chen XW, Ng CWW, Guo HW (2018) Effects of biochar on water retention and matric suction of vegetated soil. *Geotech Lett* 8(2):124–129
- Ni JJ, Leung AK, Ng CWW (2019) Modelling effects of root growth and decay on soil water retention and permeability. *Can Geotech J* 56(7):1049–1055
- Ni JJ, Bordoloi S, Shao W, Garg A, Xu G, Sarmah AK (2020) Two-year evaluation of hydraulic properties of biochar-amended vegetated soil for application in landfill cover system. *Sci Total Environ* 712:136486
- Osra FA, Ozcan HK, Alzahrani JS, Alsoufi MS (2021) Municipal solid waste characterization and landfill gas generation in Kakkia landfill, Makkah. *Sustainability* 13(3):1462
- Rogers VC, Nielson KK, Kalkwarf DR (1984) Radon attenuation handbook for uranium mill tailings cover design (No. NUREG/CR-3533; PNL-4878; RAE-18-5). Rogers and Associates Engineering Corp., Salt Lake City, UT (USA).
- Roy S, Rajesh S (2023) Tensile strength framework for unsaturated coarse- and fine-grained soils. *Int J Geomech* 23(7):04023095
- Scholl P, Leitner D, Kammerer G, Lioskandl W, Kaul HP, Bodner G (2014) Root induced changes of effective 1D hydraulic properties in a soil column. *Plant Soil* 381(1–2):193–213

- Sun Z, Moldrup P, Elsgaard L, Arthur E, Bruun EW, Hauggaard-Nielsen H, de Jonge LW (2013) Direct and indirect short-term effects of biochar on physical characteristics of an arable sandy loam. *Soil Sci* 178(9):465–473
- TDOT (Tennessee Department of Transportation) 1981 Subgrade Construction and Preparation: Specifications for Road and Bridge Construction. Tennessee Department of Transportation (TDOT) Bureau of Highways, Kingsport, TN, USA.
- van Genuchten MT (1980) A closed-form equation for predicting the hydraulic conductivity of unsaturated soils. *Soil Sci Soc Am J* 44(5):892–898
- Vergani C, Graf F (2015) Soil permeability, aggregate stability and root growth: a pot experiment from a soil bioengineering perspective. *Ecology* 9(5):830–842
- Villagra-Mendoza K, Horn R (2018) Effect of biochar addition on hydraulic functions of two textural soils. *Geoderma* 326:88–95
- Wickramarachchi P, Kawamoto K, Hamamoto S, Nagamori M, Moldrup P, Komatsu T (2011) Effects of dry bulk density and particle size fraction on gas transport parameters in variably saturated landfill cover soil. *Waste Manage* 31(12):2464–2472
- Wong JTF, Chen Z, Chen X, Ng CWW, Wong MH (2017) Soil-water retention behavior of compacted biochar-amended clay: a novel landfill final cover material. *J Soil Sediment* 17:590–598
- Wong JTF, Chen X, Deng W, Chai Y, Ng CWW, Wong MH (2019) Effects of biochar on bacterial communities in a newly established landfill cover topsoil. *J Environ Manag* 236:667–673
- Wong JTF, Chow KL, Chen XW, Ng CWW, Wong MH (2022) Effects of biochar on soil water retention curves of compacted clay during wetting and drying. *Biochar* 4(1):4
- Yan S, Zhang S, Yan P, Aurangzeib M (2022) Effect of biochar application method and amount on the soil quality and maize yield in Mollisols of Northeast China. *Biochar* 4(1):56
- Yang B, Li D, Yuan S, Jin L (2021) Role of biochar from corn straw in influencing crack propagation and evaporation in sodic soils. *CATENA* 204:105457
- Zettwoog P, Fourcade N, Campbell FE, Caplan H (1982) The radon concentration profile and the flux from a pilot-scale layered tailings pile.
- Zhan LT, Qiu QW, Xu WJ, Chen YM (2016) Field measurement of gas permeability of compacted loess used as an earthen final cover for a municipal solid waste landfill. *J Zhejiang Univ Sci A* 17(7):541–552
- Zhang Y, Gu K, Li J, Tang C, Shen Z, Shi B (2020) Effect of biochar on desiccation cracking characteristics of clayey soils. *Geoderma* 364:114182
- Zhao B, Santamarina JC (2020) Desiccation crack formation beneath the surface. *Géotechnique* 70(2):181–186
- Zornoza R, Moreno-Barriga F, Acosta JA, Muñoz MA, Faz A (2016) Stability, nutrient availability and hydrophobicity of biochars derived from manure, crop residues, and municipal solid waste for their use as soil amendments. *Chemosphere* 144:122–130

Submit your manuscript to a SpringerOpen[®] journal and benefit from:

- Convenient online submission
- Rigorous peer review
- Open access: articles freely available online
- High visibility within the field
- Retaining the copyright to your article

Submit your next manuscript at ► [springeropen.com](https://www.springeropen.com)
